Spatiotemporal Brain Imaging: Microscopic&Systems Level (EB00790).

Overall goals and objectives

The advent of non-invasive imaging methods such as functional magnetic resonance imaging (fMRI) has made it possible to obtain spatial maps of hemodynamic "activation" in the human brain under a variety of conditions. However, the indirect and poorly understood nature of the coupling between these hemodynamic signals and the underlying neuronal activity has greatly limited the interpretability of neuroimaging results in terms of the underlying biophysics and cellular organization of the brain at the microscopic scale. The overall goal of this project is to develop an integrated suite of technologies to bridge this critical gap. To this end, we have been working in parallel on improving the spatial and temporal domains of MRI and optical imaging technologies, and on applying these developments to study neurovascular coupling in the somatosensory cortex. Finally, during the past year, we have commenced application of newly developed technological tools to clinically-related experiments. Below is the summary of the progress on each of the aims during the funding year 2004/2005.

Improvement of fMRI spatial resolution

RF coil arrays for brain imaging in primates

Bring MRI to the spatial level where columnar and laminar structures can be studied and compared to invasive measurements, requires increased detection efficiency, addressed by the RF coil development. Phased arrays of small surface coils extend the high sensitivity detection of small surface coils to substantially larger regions, including bilateral coverage of the brain. The phased array extends the coverage and sensitivity of surface coils by simultaneously receiving the MR signals from multiple small independent coils, each designed to optimize the SNR in a small region adjacent to the coil. During the past year we have developed an 8-channel phased-array RF coil for non-human primate imaging at 3T and used this coil to acquire high SNR data in anesthetized macaques. Our 8-channel phased-array coil consists of seven coils, which are arranged symmetrically around the head covering the frontal lobe, the temporal lobe, and the occipital lobe. An additional coil is mounted horizontally on top.

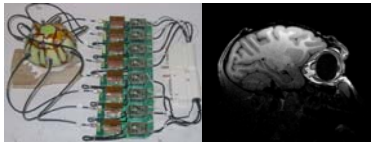

Figure 1. Primate 8-channel phased-array coil.

Ex-vivo diffusion imaging of primate brain provides a bridge between in vivo MRI and histological analysis. Most of our knowledge of brain anatomy is obtained using fixed tissue samples. Using MRI-based histology one can avoid reconstruction from single slices. In addition, since fixation procedure does not cause a change in fiber *orientation*, DTI scalar anisotropy indices are preserved.

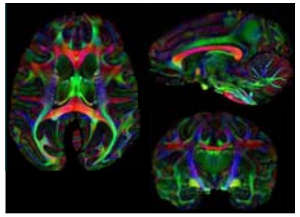

Figure 2. Primate Diffusion Tensor Imaging (DTI). Adult primate brain specimens were immersion fixed in formalin, and soaked 2 weeks in PBS/GdDTPA. This treatment results in decrease of T1 and increase in T2.
The brains were scanned at 4.7*T*, 3D SE-DTI, bmax=4000, TR ~200-400ms.
We used isotropic resolution of 440 and 120 μm for DTI and structural scans respectively.

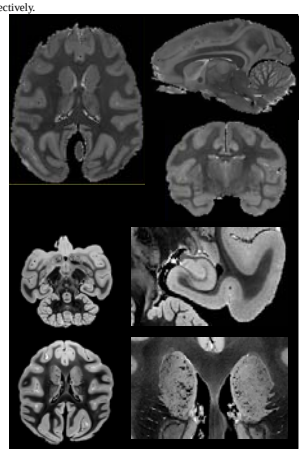

Figure 3. Primate *ex-vivo* structural imaging.

Co-investigators:

MRI: **Lawrence Wald, Bruce Rosen, Helen D'Arceuil, Alex de Crespigny**

Optical Imaging of the functional response: **David Boas, Elizabeth Hillman**

Optical imaging of vascular microstructure: **David Kleinfeld, Philbert Tsai**

Neurovascular coupling: **Anna Devor**

Improvement of the spatiotemporal resolution of optical imaging

Optical Coherence Tomography (OCT) as a tool for functional brain imaging

Depth resolution is a limitation of the optical methods primarily used to date. During the past year we have been developing optical coherence tomography (OCT) that provides depth resolution is sensitive to light scattering.

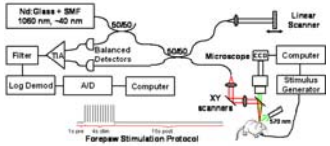

Figure 4. Simultaneous video microscopy and OCT setup. The video microscopy method was used to localize and characterize the functional activation region for placement of the OCT beam. We used a time domain OCT system with dual-balanced detection and log demodulation. This system operates at 1060 nm center wavelength using an Nd:Glass laser outputting ~ 100 fs pulses. The laser is coupled into a standard HI-1060 single mode fiber and nonlinear effects in the single mode fiber broaden the optical spectrum to ~ 40 nm, which results in an axial resolution of ~18 μm in air (13 μm in tissue). The source is split by two 3dB couplers into a reference and a sample arm. Reference delay scanning is performed at ~1150 Hz and images of ~ 380 transverse pixels are acquired at 3 frames per second. The beam is positioned on the sample using a x-y scanning pair of galvanometers. A single 60 mm focal length lens is used after the collimating lens to provide a lateral spot size of ~40 μm. The focusing OCT beam is redirected onto the sample using a hot mirror which allows visible light to pass while reflecting infrared. This configuration has the advantage of allowing easy interface with the existing video microscopy system. Measured system sensitivity from a single high reflector was > 95 dB with ~ 14 mW illumination on the sample.

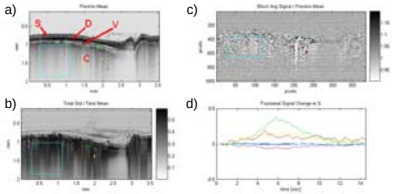

Figure 5. OCT functional imaging in rat somatosensory cortex. a) The thinned skull (S) appears patchy with a highly scattering layer thought to be the dura separating it from the sub-arachnoid space and the cortex (C). Large surface cortical vessels (V) can be seen clearly. **b)** physiologic noise during the 20 min data collection run by plotting the standard deviation divided by mean intensity at every pixel. **c)** OCT functional signal is computed by dividing each time point in the stimulus and post-stimulus periods by the mean of the pre-stimulus period (electrical forepaw stimulation). The shape of the OCT response correlates well with video microscopy suggesting that this OCT signal may reflect changes in red blood cell density, although neuronal swelling can not be ruled out at this point.

All-optical histology: Reconstruction of vascular micro-architecture

We used two-photon laser scanning microscopy in conjunction with fluorescent labeling for quantitative reconstruction of neuronal and vascular architectonics in rodent brain. Our all-optical histology method allows to automatically map, in three dimensions, the location and size of cell nuclei concurrent with the position of the blood vessels in cortex.

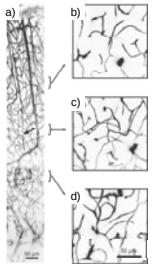

Figure 6. Vascular reconstruction. a) Maximal side projection from image stack from sensory cortex of mouse perfused with fluorescein/dextran/agarose, pre-treated with Triton X-100 and cleared with sucrose. Contrast in the images is inverted for greater detail visualization. **b-d)** Maximal x-y projections over 50 μm taken from subsets (brackets) of data in a).

Fluorescein labeling of lumen of blood vessels allows full reconstruction of vascular micro-architecture within a cortical column at micrometer precision in three dimensions.

Nuclei of all cells can be labeled by a DNA stain Hoechst 33342. NeuN-conjugated rhodamine can be used simultaneously with Hoechst to label only neuronal nuclei. Combining of Hoechst 33342 and NeuN with fluorescein lumen labeling of blood vessels allows to quantify the three dimensional distribution of neuronal and nonneuronal cells, and vessels in the brain without a priori statistical assumptions.

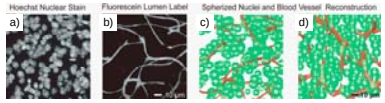

Figure 7. Nuclear and vascular labeling co-localized in mouse cortex. a-b) Maximal projection through simultaneously recorded fluorescent channels that respond primarily to Hoechst 33342 and fluorescein. The images are projected through a depth of 50 μm. **c-d)** Projected views through the x-y and x-z planes of the reconstructed images. Vessels are colored red and nuclei 60% transparent green.

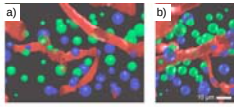

Figure 8. Triple-reconstruction of neuronal nuclei, nonneuronal nuclei and vasculature. Hoeshst 33342 and NeuN were used to label all nuclei and neuronal nuclei respectively.

a-b) Projected view along the x-y and x-z planes of 200 μm deep reconstructed volume. Vascular = red, neuronal = green, glial = blue.

Application of new technologies to image functional activation

Application of Laminar Optical tomography (LOT) to imaging of hemodynamics

We have applied a new method called Laminar Optical Tomography (LOT), that has been developed in our group in the funding year 2003/2004, for depth-resolved study of hemodynamic activation in rat somatosensory cortex. We image the cortex in 3D to depths of ~2mm with 100-200 micron resolution, making multiple dual-wavelength measurements. 3D evolution of cortical hemodynamic activation was computed from LOT data. Moreover, we were able to reliably extract vascular compartment-specific hemodynamic signals.

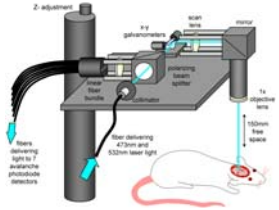

Figure 9. Diagram of LOT system. Optics are similar to a confocal microscope. 473nm and 532nm interlaced laser light is delivered by a fiber, collimated, and passed through a polarizing beam splitter onto x and y scanning galvanometer mirrors. The beam then passes through a scan lens and an objective lens to focus onto the surface of the thinned skull of the rat. Scattered light passes back through this optical system, is de-scanned by the galvanometers, is reflected off the polarizing beam splitter, passes through a lens and falls onto a linear fiber bundle. Light collected by each fiber in the bundle is transmitted to one of 7 avalanche photodiode detectors. The fiber at the center of the bundle collects confocal light. Fibers offset from the optical axis of the system collect scattered light emerging from the brain at different distances away from the scanning focused beam. The wider the separation between the beam's focus and the detection position, the deeper the detected light have traveled into the cortex.

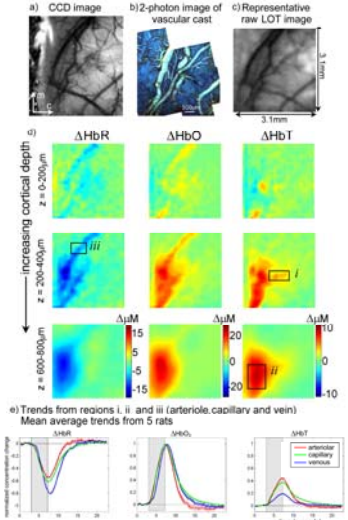

Figure 10. Depth-resolved hemodynamic imaging using LOT. a) CCD image of rat cortical surface through thinned skull, **b)** 2-photon image of fluorescent vascular cast of the same rat (ex-vivo), **c)** a representative raw LOT image of the same region. **d)** depth-resolved LOT images of deoxy-, oxy- and total hemoglobin concentration changes in the cortex 0.6 seconds after cessation of a 4 second forepaw stimulus. **e)** the time-courses in deoxy-, oxy and total hemoglobin concentration changes corresponding to the voxels isolated in the LOT images above (labeled **i**, **ii** and **iii**). These regions are hypothesized to represent arterial, capillary and venous contributions respectively.

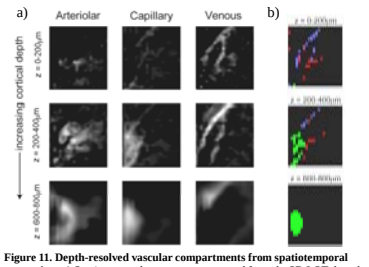

Figure 11. Depth-resolved vascular compartments from spatiotemporal separation: a) Spatiotemporal components extracted from the 3D LOT data shown in figure 10. Gray scale represents the amplitude of the component in each voxel that varies according to the arterial, capillary and venous functional time-courses shown in figure 10. By isolating deoxy-, oxy- and total hemoglobin temporal characteristics of each vascular compartment, we have isolated the 3D spatial extent of the regions that correlate with the temporal behavior. **b)** the result of objective time-course general characteristic masking, where voxels in the raw LOT data were searched to identify regions that had only the basic temporal characteristics of each vascular compartment.

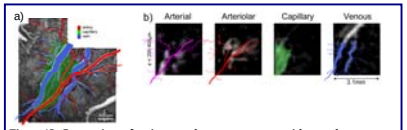

Figure 12. Comparison of active vascular compartments with vascular architecture. Correlation between LOT functional vascular compartments and vascular architecture. **a)** 2-photon image stack of fluorescent vascular cast of rat. Veins (blue) and arteries (red) are easily identified from their smoothness, their direction and by following their branches. **b)** superficial slice (200-400 μm) of 3D vascular compartment image from LOT showing spatial components corresponding to extracted vascular compartment functional time courses, including the 4th spatiotemporal component (arterial). The tracing of the arteries and veins from the vascular cast was rotated, scaled and overlaid onto the LOT results. The capillary response was traced from the LOT results then transformed and overlaid onto the vascular cast image (green).

Comparison of a spatial profile of neuronal and hemodynamic signals

During brief single-vibrissa stimulation there is a spatially biphasic hemodynamic response consisting of regions of maximal activation surrounded by activation that is opposite in sign. We do not observe a similar biphasic spatial pattern in neuronal activity measured using voltage-sensitive dyes (VSD). Our results show that: (1) the surround "negative" hemodynamic activation is not mediated by neuronal inhibition, and (2) the spatial spread of center "positive" hemodynamic activity measured with roughly co-localizes with neuronal activation.

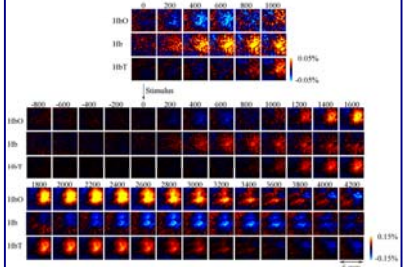

Figure 13. Spatiotemporal evolution of the hemodynamic reponse. Full field time series of deoxy-, oxy and total hemoglobin signals in response to a deflection of a single whisker (calculated from 6 wavelengths data). Each image represents an individual frame (average of ~1400 trials). Time between consecutive images is 200 msec. The signal is expressed in percent change relative to baseline concentration. The arrow denotes stimulus delivery. The time period of the initial dip is repeated on a different intensity on top.

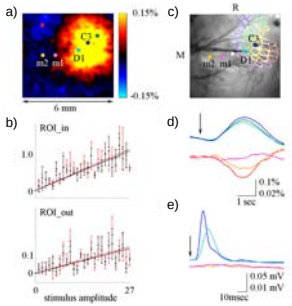

Figure 14. The hemodynamic response has an antagonistic center-surround spatial pattern. a) an image of oxyhemoglobin at the peak of the response. **b)** integral oxy- (red) and total hemoglobin (black) responses as a function of stimulus intensity in the center (principal barrel, ROI_in) and surround (>3mm away from the recording electrode, ROI_out). Data from 5 animals were averaged, all amplitudes are shown. The error bars reflect the inter-subject standard error. **c)** the locations of electrophysiological recordings are superimposed on the image of the vasculature corresponding to the functional map in a). Recordings from locations m1 and m2 were performed following recordings from C3 and D1 barrels. **d)** timecourses of HbT response averaged from 300x300 μm ROIs around recording electrodes. The locations are color coded in a) and c). **e)** MUA recorded from the locations marked in c). Responses to 7 largest stimulus amplitudes are averaged in d) and e). The vertical scale for the top and bottom plots in d) and e) differ by factor of 5. The arrow denotes stimulus delivery.

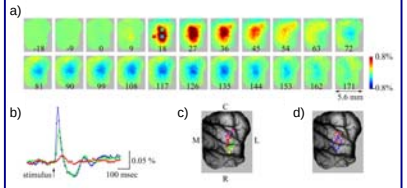

Figure 15. VSD imaging of a neuronal response to a single whisker deflection. a) full-field imaging of the neuronal response to a single deflection of one whisker. Each image represents a single frame, an average of 100 trials. **b)** timecourses extracted from areas of 500x500 mm marked by squares in A (t=18). The traces are color coded. **c)** an image of the exposed cortex. Electrode penetration sites are marked by dots. The color indicates the principal whisker. M medial, L lateral, R rostral, C caudal. **d)** 60% contour plots for stimulation of two neighboring whiskers at18 msec following the stimulus onset.